Chemical Geology 501 (2018) 19–25

Contents lists available at ScienceDirect

Chemical Geology

journal homepage: www.elsevier.com/locate/chemgeo

Experimental determination of the viscosity of Na_2CO_3 melt between 1.7 and 4.6 GPa at 1200–1700 °C: Implications for the rheology of carbonatite magmas in the Earth's upper mantle

Vincenzo Stagno[a,*], Veronica Stopponi[a], Yoshio Kono[b], Craig E. Manning[c], Tetsuo Irifune[d,e]

[a] Department of Earth Science, Sapienza University of Rome, Italy
[b] HPCAT, Geophysical Laboratory, Carnegie Institution of Washington, IL, USA
[c] Department of Earth, Planetary and Space Sciences, University of California, Los Angeles, USA
[d] Geodynamic Research Center, Ehime University, Japan
[e] Earth-Life Science Institute, Tokyo Institute of Technology, Tokyo, Japan

ARTICLE INFO

Editor: D.B. Dingwell

Keywords:
Na_2CO_3 melt
Carbonatites
Viscosity
Paris-Edinburgh press
Carbon cycle
Mantle melting

ABSTRACT

Knowledge of the rheology of molten materials at high pressure and temperature is required to understand magma mobility and ascent rate at conditions of the Earth's interior. We determined the viscosity of nominally anhydrous sodium carbonate (Na_2CO_3), an analogue and ubiquitous component of natural carbonatitic magmas, by the in situ "falling sphere" technique at 1.7, 2.4 and 4.6 GPa, at 1200 to 1700 °C, using the Paris-Edinburgh press. We find that the viscosity of liquid Na_2CO_3 is between 0.0028 ± 0.0001 Pa·s and 0.0073 ± 0.0001 Pa·s in the investigated pressure-temperature range. Combination of our results with those from recent experimental studies indicate a negligible dependence on pressure from 1 atm to 4.6 GPa, and a small compositional dependence between molten alkali metal-bearing and alkaline earth metal-bearing carbonates. Based on our results, the viscosity of Na_2CO_3 is consistent with available viscosity data of both molten calcite (determined at high pressure and temperature) and Na_2CO_3 at ambient pressure. Molten Na_2CO_3 is a valid experimental analogue for study of the rheology of natural and/or synthetic near-solidus carbonatitic melts. Estimated values of the mobility and ascent velocity of carbonatitic melts at upper conditions are between 70 and 300 g cm^{-3}·Pa^{-1}·s^{-1} and 330–1450 m·$year^{-1}$, respectively, when using recently proposed densities for carbonatitic melts. The relatively slow migration rate allows magma-rock interaction over time causing seismic anomalies and chemical redox exchange.

1. Introduction

The percolation of CO_2-rich magmas has played an important role in modifying the composition of the mantle lithosphere, creating seismic low-velocity zones, and transferring volatiles from Earth's interior to its atmosphere over time (Chantel et al., 2016; Keller et al., 2017; Stagno et al., 2013). Experimental studies on melting of synthetic carbonated mantle rocks have provided important chemical and mineralogical constraints on the amount of carbon dissolved in the originated melts (Dalton and Wood, 1993; Dalton and Presnall, 1998; Gudfinnsson and Presnall, 2005; Dasgupta and Hirschmann, 2010), element distribution coefficients to determine the melt fractions (Dasgupta et al., 2009), and redox reactions that are essential to explain the origin of diamonds (Stagno and Frost, 2010; Rohrbach and Schmidt, 2011). However, understanding these processes also requires information on the time during which rock and melt can interact, as controlled by the rheology and migration rates of CO_2-rich magmas at depth.

Experimental study of the rheology of carbonatite liquids is plagued by problems associated with the choice of appropriate analogue material. The chemical composition of natural mantle carbonatites may be influenced by late-stage processes such as fractional crystallization and wall rock assimilation. It is thus problematic to employ natural carbonatite rock compositions. On the other hand, use of synthetic systems that approach natural compositions in complexity is difficult due to the tendency of the liquids to crystallize and/or loose CO_2 upon quench during initial preparation (Genge et al., 1995). Investigations of the rheological properties of carbonatitic melts at mantle conditions have therefore typically employed highly simplified, analogue compositions like pure carbonates. Fig. 1 shows the pressure and temperature conditions of previous studies including those discussed here with viscosity

* Corresponding author.
E-mail address: vincenzo.stagno@uniroma1.it (V. Stagno).

https://doi.org/10.1016/j.chemgeo.2018.09.036
Received 22 March 2018; Received in revised form 14 August 2018; Accepted 29 September 2018
Available online 05 October 2018

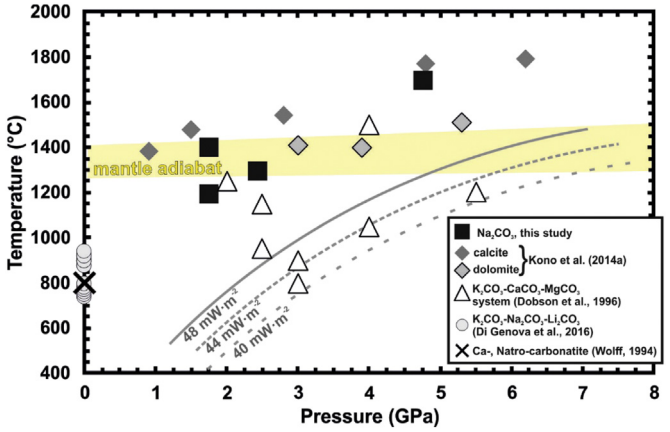

Fig. 1. Diagram showing temperatures and pressures set for the experiments of this study compared to previous studies, plotted along with the mantle adiabat and Archaean cratonic geotherms.

data ranging from 750 °C up to almost 1800 °C at pressures between 1 atm and 6.2 GPa, and employing simplified compositions such as $K_2Mg(CO_3)_2$ and $K_2Ca(CO_3)_2$ (Dobson et al., 1996), and dolomite and calcite (Kono et al., 2014a), as analogue of natural carbonatitic magmas. Viscosity values for molten calcite and dolomite estimated by Kono et al. (2014a) using the falling sphere technique (Maude, 1961; Kanzaki et al., 1987) combined with ultrafast in situ X-ray imaging are between 0.006 and 0.01 Pa·s (Table 1). However, some compositions resulted in higher melting temperatures than expected for near-solidus melts at the P-T conditions relevant for the mantle adiabat (Fig. 1). In contrast, the starting material used by Dobson et al. (1996) allowed performing measurements at lower temperatures representative of Archaean cratons (Fig. 1); their proposed viscosities resulted to be up to one order of magnitude higher but were overestimated due to the low recording time (40 frame per second).

In this study, we used Na_2CO_3 to investigate the effect of alkali metal compositions on the viscosity of carbonatitic melts. Na_2CO_3 is an important component of complex natural carbonatitic melts (Woolley and Kjarsgaard, 2008), as testified by natrocarbonatites erupted at Ol Doinyo Lengai (Tanzania), Na-rich carbonate inclusions in kimberlite-hosted mantle xenoliths (Na_2O up to 34.3 wt%; Giuliani et al., 2012), and Na-carbonate-bearing inclusions in fibrous diamonds (6.58 wt% Na_2O vs. 16.99 wt% CaO, Kopylova et al., 2010, up to 9.5 wt% Na_2O vs. 29 wt% CaO, Shiryaev et al., 2005). Recent studies used Na_2CO_3 to investigate the reactivity of CO_2-rich melts by mineral assimilation (Russell et al., 2012), and to determine the viscosity of natrocarbonatites at ambient pressure (Di Genova et al., 2016; Table 1). The Na_2CO_3 was used in experimental studies on the dissolution of mantle minerals to explain the origin and emplacement of kimberlitic rocks (Kamenetsky and Yaxley, 2015) considering that carbonatites have been proposed to be parental of kimberlitic melts (Kamenetsky et al., 2013, 2014). Importantly, carbonate melts at depths have been experimentally demonstrated to be Ca-, Mg- rich, Fe- rich. However, phase relations explored accurately by adding Na_2O like in the CMASFN + CO_2 and CMASN + CO_2, systems by Litasov and Ohtani (2009a, 2009b, 2010); Litasov et al. (2013, 2014) showed that near solidus melts can contain even up to 18.89 wt% of Na_2CO_3 component vs. 19.13 wt% $CaCO_3$ within a single produced carbonatitic melt. Recently, Thomson et al. (2016) emphasized the important role of Na_2CO_3 in lowering the melting temperature of a carbonated subducted slab with formation of Na-rich carbonate melts (up to 15.24 wt% Na_2O versus 22.85 wt% CaO in the reported RUN #3) that eventually will limit the subduction of carbon further in the lower mantle. These experimental studies supported by the frequent presence of Na both in melt inclusions

Table 1
Experimental studies on viscosity of carbonated compounds that have been considered representative of carbonate-rich melts by the authors.

Composition, references	Pressure (GPa)	Temperature (°C)	Viscosity (Pa·s)
Ca-carbonatite, Wolff (1994)	0.0001	800	0.08
Natrocarbonatite, Wolff (1994)	0.0001	800	0.008
$K_2Mg(CO_3)_2$, Dobson et al. (1996)	3.0	800	0.036 (± 0.019)
	3.0	900	0.022 (± 0.010)
	5.5	1200	0.006 (± 0.003)
$K_2Ca(CO_3)_2$, Dobson et al. (1996)	2.5	950	0.032 (± 0.019)
	2.5	1150	0.018 (± 0.011)
	4.0	1050	0.023 (± 0.013)
25 wt% $MgCO_3$–75 wt% K_2CO_3, Dobson et al. (1996)	2.0	1250	0.065
K_2CO_3, Dobson et al. (1996)	4.0	1500	0.023
REE-rich carbonatite, Dobson et al. (1996)	3.0	530	0.155 (± 0.065)
Calcite ($CaCO_3$), Kono et al. (2014a, 2014b)	0.9	1380	0.0067 (± 0.0006)
	1.5	1480	0.0062 (± 0.0003)
	2.8	1540	0.0059 (± 0.0004)
	4.8	1770	0.006 (± 0.0003)
	6.2	1790	0.0061 (± 0.0004)
Dolomite ($(Mg_{0.40}Fe_{0.09}Ca_{0.51})CO_3)_2$, Kono et al. (2014a, 2014b)	3	1410	0.0099 (± 0.0007)
	3.9	1400	0.0084 (± 0.0008)
	5.3	1510	0.0087 (± 0.0007)
Double-layered probing sphere measured for dolomite, Kono et al. (2014a, 2014b)	No data	1360	0.0117 (± 0.0007)
	2.9	1490	0.007 (± 0.0005)
K_2CO_3, Di Genova et al. (2016)	0.0001	910	0.0038
	0.0001	930	0.0036
Na_2CO_3, Di Genova et al. (2016)	0.0001	880	0.0049
	0.0001	900	0.0047
	0.0001	880	0.0067
Li_2CO_3, Di Genova et al. (2016)	0.0001	740	0.0142
	0.0001	750	0.0136
	0.0001	760	0.0132
	0.0001	770	0.0129
	0.0001	780	0.0125
	0.0001	800	0.0121

Notes: uncertainties written in italics were obtained from Fig. 5 in Dobson et al. (1996). No uncertainties are provided by Di Genova et al. (2016), although it is claimed to be smaller than the symbol size in their Fig. 4 (i.e. < ± 0.001). No uncertainties are available for Wolff (1994) data.

of fibrous diamonds (Kopylova et al., 2010) and in natural carbonatites (Woolley and Kjarsgaard, 2008) implies a critical role of alkali metals dissolved into carbonatitic melts in lowering further their viscosity affecting, then, their migration rate. The high concentration of Na_2O of these melts is expected to affect their viscosity and, in turn, the kinetics of the reactions between these melts and the surrounding reduced mantle. At mantle conditions, Na_2CO_3-dominated melts are interconnected in fine-grained rocks at low melt fractions of 0.05 wt% (Minarik and Watson, 1995; Watson et al., 1990), and that these melts can percolate rapidly upward through polycrystalline mineral assemblages over long distances (Hammouda and Laporte, 2000).

To date, no viscosity measurements have been performed on Na_2CO_3 liquids at pressure and temperature conditions relevant for the Earth's upper mantle that would allow modeling their ascent rate and provide insights on the effect of alkali on the viscosity of carbonatitic magmas. We determined the viscosity of Na_2CO_3 liquids in situ at upper mantle pressures and temperatures. By combining our results with previous work, we show that low viscosity leads to elevated carbonate liquid mobility, but that ascent rates are low when appropriate rock parameters are taken into account. The results provide improved understanding of carbonatite liquid migration in the mantle.

2. Experimental methods

The starting material used in this study is anhydrous Na_2CO_3 (Puratronic®, purity of 99.997%) permanently stored in a desiccator to minimize contamination from moisture. A cylindrical graphite capsule with diameter of 1.2 mm and 2.0 mm of height was filled with the Na_2CO_3 crystalline powder. Except for the run at 4.6 GPa, we used double-layered probing sphere configuration (Terasaki et al., 2001) using a small cup filled with $CaCO_3$ (calcite, Puratronic®, purity of 99.999%; Fig. 2) powder, which because of its higher melting T, delays the release of the probing sphere. Two small platinum spheres with diameter of 0.038–0.113 mm (Table 2) were placed in the center portion of the capsule and the lid, respectively. The capsule was then enclosed in a cell assembly, surrounded by a boron nitride (BN) outer capsule, graphite heater, MgO sleeve as pressure medium, ZrO_2, a rounded boron epoxy gasket as thermal insulator, and a plastic (Lexan) ring. Details on the cell assembly used in this study can be found in Kono et al. (2014b). The in-situ viscosity measurements were performed using the falling sphere technique at 16 BM-B HPCAT beamline of the Advanced Photon Source (Argonne, Illinois, USA) (Kono et al., 2014b) equipped with the Paris-Edinburgh press (Besson et al., 1992; Klotz et al., 2004). The loaded cell was first compressed to the target pressure by a hydraulic system connected to the Paris-Edinburgh press. The pressure was monitored by the equation of state (EOS) of the Pt and MgO (Kono et al., 2010) determined both collecting X-ray diffraction patterns on the metal spheres and cell parts. After compression at 1.7, 2.4 and 4.6 GPa, the sample was heated quickly (~100 °C/s) and the temperature estimated using a power vs. temperature calibration curve reported by Kono et al. (2014b) and the melting temperature of $CaCO_3$ and Na_2CO_3 (Irving and Wyllie, 1975; Li et al., 2017; Shatskiy et al., 2015; Suito et al., 2001). The temperature uncertainty is ± 50 °C similar to Kono et al. (2014b) due to combination of power vs T calibration and T change during sphere decent.

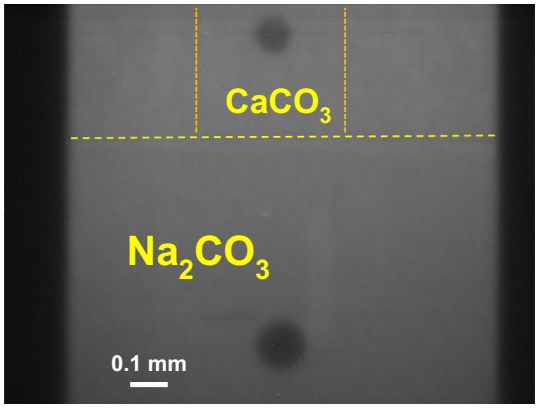

Fig. 2. Radiographic image showing the location of the two Pt spheres in the experiment at 1.7 GPa.

Experimental measurements of the viscosity were performed using unfocused white X-ray beam with radiographic images captured by a high-speed camera (Photron FASTCAM SA3) with 500 frames per second (f.p.s.) recording time. The radiographic images were collected during heating of the run until the fall of the sphere could be observed. Fig. 2 is a radiographic image showing the initial position of the Pt spheres in the middle part of the Na_2CO_3 starting sample, and inside the graphite cap at the top of the capsule embedded in $CaCO_3$ powder. Because the melting T of calcite is higher than that of Na_2CO_3, this technique allows determination of the viscosity of the liquid at two different temperatures. In our run, the fall of the Pt sphere from the middle portion of the capsule never reached terminal velocity, likely owing to the initially slow heating when approaching the Na_2CO_3 melting temperature. Therefore, our results were obtained using the top Pt sphere. The falling sphere velocity, necessary to determine the viscosity using Stokes equation, was determined from the collected radiographic images with the Tracker plugin in the ImageJ software. The diameter of the Pt spheres was measured by X-ray radiography using a high-resolution camera with a pixel size of 0.945 mm (0.850 mm for the run at 4.6 GPa) per pixel (Kono et al., 2014b). Viscosities were calculated from the falling sphere velocity determined from the radiographic images (500 f.p.s.) and Stokes law,

$$\eta = \frac{g d_s^2 (\rho_s - \rho_l)}{18 \upsilon} \frac{F}{E} \quad (1)$$

Eq. (1) includes correction factors for the effect of the wall (F) and for the end effect (E),

$$F = 1 - 2.104\left(\frac{d_s}{d_l}\right) + 2.09\left(\frac{d_s}{d_l}\right)^3 - 0.95\left(\frac{d_s}{d_l}\right)^5, \quad (2)$$

and

$$E = 1 + \frac{9 d_s}{82 Z} + \left(\frac{9 d_s}{82 Z}\right)^2 \quad (3)$$

where ν is the terminal velocity ($mm \cdot s^{-1}$) of the probing sphere calculated by tracking the Pt sphere from the radiographic images (see Supplemental Materials), ρ_s and ρ_l are the densities ($g \cdot cm^{-3}$) of the Pt sphere at high P and T (Dorogokupets and Dewaele, 2007) and melt, respectively; d is the diameter (in mm) of the sphere determined from radiographic image (pixel resolution of 0.850 and 0.945 μm/pixel), Z is the total height of the molten sample (i.e. height of the capsule of 2 mm). A fixed value of 2 g cm^{-3} was chosen for the density of molten Na_2CO_3 (Liu and Lange, 2003); however, a difference up to ± 1 g cm^{-3} (an extreme case) would not produce any considerable effect on the calculated viscosity being this < 0.001 Pa·s. Importantly, whether the two compositions (starting material and calcite) should mix, this would not interfere with the initial composition of our liquid due to the low fractions involved (< 10 vol%), and the short duration of the experiment (Table 2). However, we cannot exclude that softening/melting of Na_2CO_3 triggered softening/melting of calcite at lower temperature than expected. For this reason, our viscosity results are strictly applicable to temperatures at which both Na_2CO_3 and $CaCO_3$ are molten at the estimated pressure. Finally, experiments were quenched by shutting down the electrical power to the heater.

Table 2
Parameters for viscosity calculations.

Composition	Pressure (GPa)	Temperature (°C)	Pt sphere Ø (mm)	Falling Time (s)	Terminal velocity (mm/s)	Viscosity (Pas)
Na_2CO_3	1.7	1200	0.091	0.17	12.71	0.0049 (± 0.0001)
	1.7	1400	0.038	0.22	4.5	0.0028 (± 0.0001)
	2.4	1300	0.113	0.12	13.02	0.0073 (± 0.0001)
	4.6	1700	0.135	0.17	20	0.0045 (± 0.0000)

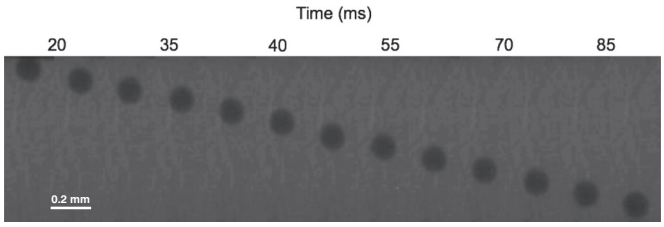

Fig. 3. X-ray radiography images of the Pt sphere in Na_2CO_3 melt as function of time for experiment at 2.4 GPa and 1300 °C.

3. Results

Run conditions and results are summarized in Table 2. Fig. 3 shows radiography images of the falling sphere with elapsed time for the run at 2.4 GPa and 1300 °C. The rapid sphere decent in these experiments narrows the terminal velocity region in the charge, thereby reducing the uncertainty in the determined viscosities to ± 0.0001 Pa·s (one sigma), which is lower than that of Kono et al. (2014a, 2014b) (Fig. S2, S4 and S8 of Supplementary Materials). With this uncertainty, the determined Na_2CO_3 melt viscosities are 0.0049 Pa·s at 1200 °C and 1.7 GPa, 0.0073 Pa·s at 1300 °C and 2.4 GPa, and 0.0045 Pa s at 1700 °C and 4.6 GPa. At 1.7 GPa and 1400 °C, we obtained a viscosity of 0.0028 Pa·s based on the fall of another small sphere attached at the top of capsule at higher temperature of 1400 °C, which confirms that the increase of temperature decreases the viscosity of molten carbonates.

4. Discussion

4.1. Effect of pressure and temperature on the viscosity of molten carbonates

Viscosity data obtained in this study using the in-situ falling sphere technique can be compared with the viscosity determined from previous studies on different carbonate compositions. Table 1 summarizes all the results on viscosity of different molten carbonates available in literature. As illustrated in Fig. 4, our results at 1200–1700 °C and 1.7–4.6 GPa yield viscosities of ~0.003 to ~0.007 Pa·s, which are comparable to or lower than all previous results obtained at high pressure and temperature. In particular, runs at 1.7 GPa/1200 °C and 2.4 GPa/1300 °C fall within the range of 0.0047–0.0069 Pa·s measured at ambient pressure on molten Na_2CO_3 by Di Genova et al. (2016) (Fig. 4a) using an improved rheometer capable of performing measurements under controlled CO_2-rich atmosphere. This interval also includes the viscosity data for molten calcite by Kono et al. (2014a) at pressures between 0.9 and 6.2 GPa where almost no pressure dependence was observed, and that of $K_2Mg(CO_3)_2$ of 0.006 at 5.5 GPa and 1200 °C proposed by Dobson et al. (1996) although likely overestimated. The lowest viscosity of 0.0028 Pa·s was determined at 1.7 GPa and 1400 °C for Na_2CO_3 liquid, even lower than the viscosity of K_2CO_3 liquid measured at ambient pressure (Di Genova et al., 2016), as well as the viscosity data at 4.6 GPa/1700 °C (0.0045 Pa·s) that also falls below the viscosity trend at ambient pressure. The high viscosities reported by Dobson et al. (1996) for K_2CO_3, K_2CO_3-$MgCO_3$ and K_2CO_3-$CaCO_3$ melts, and by Wolff (1994) Ca-carbonatite, although overestimated, likely still indicate a strong temperature dependence for

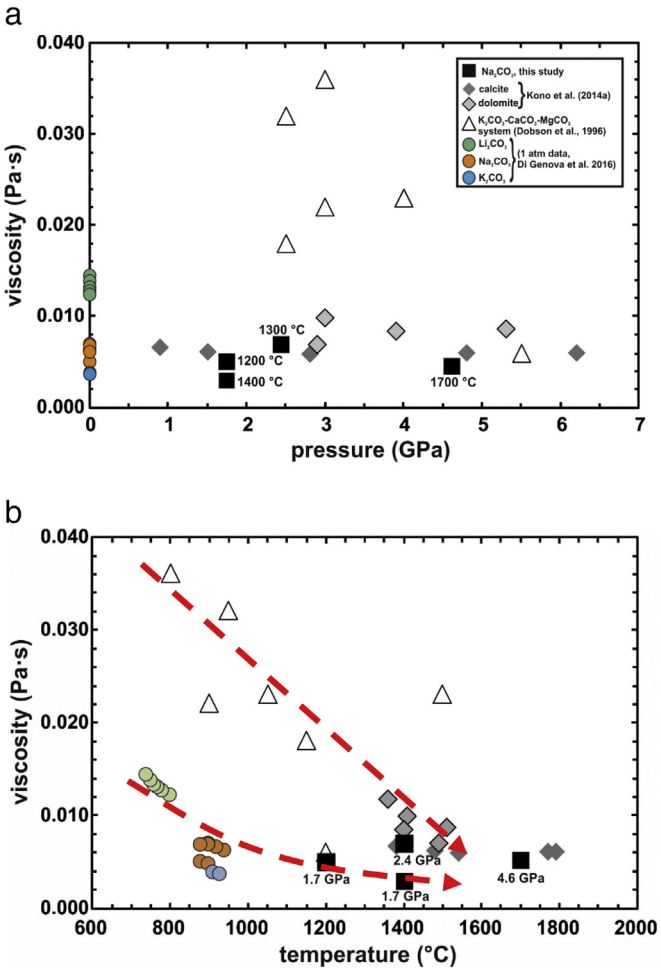

Fig. 4. Shown is the viscosity plotted as a function of (a) pressure and (b) temperature. Data from literature are reported for comparison with available uncertainties shown in Table 1. White triangles refer to experiments performed with $K_2Ca(CO_3)_2$, $K_2Mg(CO_3)_2$ and K_2CO_3 by Dobson et al. (1996); dark and light grey diamonds are runs performed by Kono et al. (2014a, 2014b) on molten calcite and dolomite, respectively. Colored symbols are representative of 1-atm experiments by Di Genova et al. (2016), while grey and black squares are experiments described in this study. The uncertainty in our viscosity measurements is within the symbol size.

these compositions (Fig. 4b). The viscosity of K_2CO_3 at 1 atm pressure by Di Genova et al. (2016) is 1 order of magnitude lower (0.004 Pa·s at 1 atm and 910–930 °C) than that determined by Dobson et al. (1996; 0.023 Pa·s at 4 GPa and 1500 °C). It is possible that viscosities of Dobson et al. (1996) are up to one order of magnitude higher because of the limitation in the in situ falling sphere velocity measurements using early synchrotron X-ray techniques and slower recording rates (40 f.p.s. versus the latest falling sphere viscosity measurements at 1000 f.p.s.; Kono et al., 2014a, 2014b); however, this conclusion should be tempered by the absence of more recent measurements on the same compositions. Although we decided to show previous data by Dobson et al. (1996) (Fig. 4a–b and Fig. 5), their results are somehow overestimated

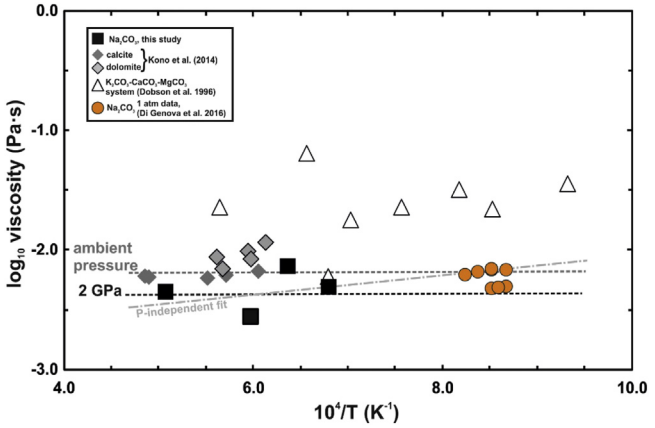

Fig. 5. Measured melt viscosities as function of reciprocal temperature for Na_2CO_3 from this study (black squares) and by Di Genova et al. (2016; orange circles,), calcite and dolomite by Kono et al. (2014a; dark and light grey diamonds, respectively), and for $K_2Ca(CO_3)_2$-$K_2Mg(CO_3)_2$ by Dobson et al. (1996; white diamonds). The three straight dashed lines are the fit to the viscosity data of molten Na_2CO_3 from this study and Di Genova et al. (2016) using a P-dependent (horizontal lines calculated at ambient P and 2 GPa) and P-independent (light grey) Arrhenius equations, respectively.

and will not be used for fitting.

Fig. 4b shows the effect of temperature on the viscosity, as determined in this and previous studies. The decrease of the viscosity is a common feature clearly observed in all compositions investigated to date. It is notably difficult to collect isobaric data due to the pressure effect on the melting temperature of solid carbonate, and the effect that heating has on the cell assembly itself, which results in a change of the nominal target pressure. In any case, the viscosity determined at 1.7 GPa decreases from 0.005 to 0.003 Pa·s within about 200 °C. Interestingly, these data plot along the extrapolated trend of viscosity of both Li_2CO_3 and Na_2CO_3 melts reported by Di Genova et al. (2016). A gradual decrease in viscosity is observed from 800 to 1550 °C, regardless compositional differences. These trends (highlighted in Fig. 4b with the red arrows) are consistent with the negligible role played by the pressure resulting from the relatively constant interatomic distances, as inferred for calcite and dolomite melts (Kono et al., 2014a; Hudspeth et al., 2018).

Fig. 5 compares viscosities from our experiments with data from the literature in terms of the logarithm of viscosity vs. reciprocal absolute temperature, to allow fitting to the Arrhenian relation,

$$\eta = \eta_0 \bullet \exp\left(\frac{E_a + P \bullet V_a}{R(T - T_0)}\right) \quad (4)$$

where η is the viscosity in Pa·s, E_a and V_a are the activation energy (kJ·mol^{-1}), and the activation volume (cm^3·mol^{-1}), η_0 and T_0 the viscosity (Pa·s) and temperature (Kelvin) at reference condition, respectively, and T is the absolute temperature in Kelvin. Our data were fitted along with those for Na_2CO_3 collected at ambient pressure (Di Genova et al., 2016) by fixing the E_a at 28 kJ·mol^{-1} (i.e. assuming no pressure effect on the activation energy) and setting the other variables unconstrained. We obtained the following parameters η_0 = 0.0065 Pa·s, E_a = 28 kJ·mol^{-1}, V_a = 54.52 cm^3·mol^{-1} and T_0 of 1496 K as best fitting with a misfit of less than ± 0.001 Pa·s for runs at 1.7 GPa/1200 °C and 2.4 GPa/1300 °C, ± 0.002 Pa·s for runs at 4.6 GPa/1700 °C, and ± 0.003 Pa·s for runs at 1.7 GPa/1400 °C. It can be noted that both activation energy and activation volume are lower than those obtained by Kono et al. (2014a) of 305 kJ·mol^{-1} and 179 cm^3·mol^{-1}, respectively, likely as result of the different behavior of the liquid alkali carbonates with respect to calcite and dolomite melts as consequence of the effect of the ionic radius on the viscosity of molten carbonates (Di Genova et al., 2016). Finally, when our data are fitted with a pressure-independent equation with A and B fitting parameter of −2.862 and 804, respectively, this still reproduces well the results both at ambient pressure and high pressure within ± 0.0025 Pa·s.

As shown in Fig. 5, therefore, two main trends of viscosities for molten carbonates can be distinguished, mostly resulting from the different activation energy, one including Na-carbonates, and a second one including calcite, dolomite and K-Ca and K-Mg carbonate solid solutions. In contrast with the common viscosity trend exhibited by silicate liquids (Dingwell, 2006; Giordano et al., 2006), which varies within 3–4 orders of magnitude, Fig. 5 shows variations in viscosity that are smaller than 0.4 log unit for each proposed trend corresponding to a difference of < 0.005 Pa·s, well within the field of ultralow viscosity for carbonatitic melts. Further, our results appear consistent with the low viscosity measured on liquid NaCl and KCl ranging between 0.001 and 0.0027 Pa·s (Kono et al., 2013), and this can be explained as consequence of the ionic nature of carbonate liquids.

4.2. Migration rate of carbonatitic melts from the mantle source rock

The presence of small volumes of carbonatitic melts (< 0.1% in volume; Dasgupta et al., 2013) in the Earth's upper mantle has been subject of several studies aimed at understanding the origin of seismic anomalies detected beneath mid-ocean ocean ridges. Such studies were based mainly on electrical conductivity experimental models (Gaillard et al., 2008) and geophysical interpretations of the seismic anisotropy near ridge axis (Gu et al., 2005; Dunn et al., 2001; Evans et al., 1999) that show evidence of the possible presence of carbonatitic melts formed by partial melting of a carbonated garnet peridotite (Salters and Hart, 1989) anticipating the formation of large fractions of mid ocean-ridge basalts (MORBs).

Experimental studies in the last decades investigated the origin of CO_2-melts both in natural and synthetic simplified systems representative of either carbonated peridotite or eclogite mineral assemblages (Hammouda and Keshav, 2015, and references therein). The composition of quenched near-solidus melts ranged between 35 and 45 wt% CO_2 and ~zero (pure dolomitic melts) and 10 wt% SiO_2 in a pressure range of 3–27 GPa and temperatures representative of either the mantle adiabat or thermal regimes of various subducting slabs from 800 to 1800 °C. As these small melt fractions form when the local carbonated mantle rock crossed the appropriate mantle adiabat under redox conditions buffered by the surrounding silicate minerals at the carbon-carbonate level (EMOD; Eggler and Baker, 1982; Stagno and Frost, 2010), it is likely that near-solidus melts are stable within a certain depth depending on the availability of diamonds to oxidise to molten carbonate and their rheological properties before evolving towards more silica-rich melts during their ascent (Stagno et al., 2013; Stagno et al., 2015).

Following Kono et al. (2014a, 2014b), we can use our data to model the mobility and migration rate of carbonatitic melts at upper mantle conditions and estimate the difference of the obtained results for both molten carbonate of Na_2CO_3 and alkali earth metal carbonates (e.g. molten calcite and dolomite). The migration rate was calculated using the equation,

$$\phi w_0 = \frac{kg\Delta\rho}{\eta}, \quad (5)$$

with,

$$k = \frac{a^2\phi^n}{C}, \quad (6)$$

where k is the permeability, a is the characteristic grain diameter, ϕ is the melt fraction, while n (equal to 2) and C (equal to 1600) are numerical constants, g is the gravitational acceleration constant, and w_0 is the melt ascent velocity. This leads to an average mobility, $\frac{\Delta\rho}{\eta}$, of carbonatitic melts obtained in this study varying between of ~70 and

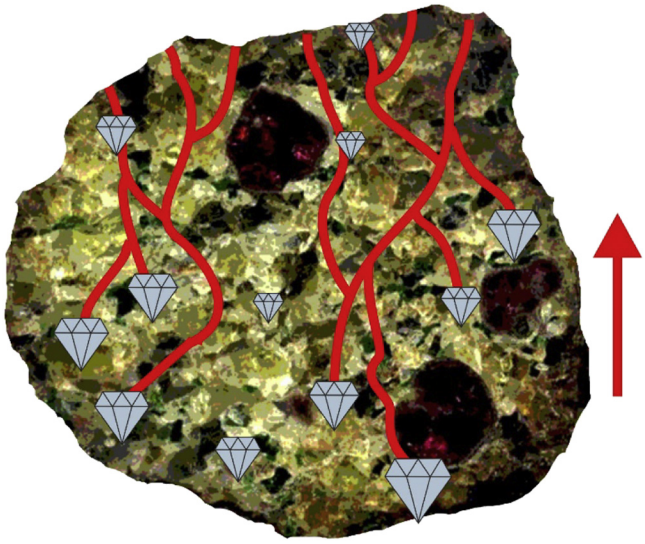

Fig. 6. Artistic representation of the redox melting of a diamond (or graphite) bearing garnet peridotite (photo courtesy of S.D. Jacobsen from the webpage http://sites.northwestern.edu/jacobsen/research-3/garnet/) chosen to represent the upper mantle by which carbonatitic melts can form and migrate upward though the hosting rock.

$300\ g{\cdot}cm^{-3}{\cdot}Pa^{-1}{\cdot}s^{-1}$ using our P-dependent fitting parameters to Eq. (4) (including the 1-atm data by Di Genova et al., 2016) for alkali carbonatitic melts and assuming Δρ (density of the solid mantle-density of pure carbonatitic melt) equal to 0.3–0.6 $g{\cdot}cm^{-3}$ at the lithosphere-asthenosphere boundary up and 1.3 $g{\cdot}cm^{-3}$ in the oceanic lithosphere, respectively (Hudspeth et al., 2018; Li et al., 2017). The calculation using Eq. (5) and Eq. (6) results in the melt ascent velocity between ~330 m/yr and 1450 m/yr using *a* of 5 mm and melt fraction of 0.001% in volume (Keller et al., 2017) over the investigated density range. These values are higher than those obtained by Kono et al. (2014a, 2014b) of ~80–115 m/yr for $CaMg(CO_3)_2$ melts owing to the different calculated mobility (i.e. the lower viscosity) and material parameters.

It has been generally proposed that most of the upper mantle would fall in the stability field of diamond due to the limited amount of oxygen with depth required to stabilize carbonate minerals and melts (Stagno and Frost, 2010; Stagno et al., 2015; Woodland and Koch, 2003). The oxidation of diamonds (C) to carbonate (CO_3^{2-}) with consequent melting can only occur as result of the oxygen provided by the surrounding Fe-bearing garnet peridotite during asthenospheric convection at about 120 km beneath mid-ocean ridges (Stagno et al., 2013). This process of redox melting is summarized in Fig. 6, and it has likely occurred over the last 3.8 Gy of Earth history (Aulbach and Stagno, 2016), even at shallower depths in response of the varying mantle thermal regime. Diamond oxidation therefore plays a major role in modulating the exchange of carbon from the interior to the atmosphere. Our results show that once carbonatitic melts are generated in the upper mantle, their stability is strongly controlled by both the local oxygen fugacity and the mobility at the time when the melt is still penetrating the source rock, prior than being in an open conduit. This relatively slow migration rate resulting from the density contrast between the mantle rock source and carbonatitic melts is a precondition that allows linking seismic anomalies with the presence of small degree of partial melts.

5. Conclusions

We determined the viscosity of molten Na_2CO_3 at 1.7, 2.4 and 4.6 GPa, at temperatures of 1200 °C–1700 °C to be 0.0028 to 0.0073 Pa·s. Our results agree with data from previous studies of molten calcite and Na_2CO_3 (Kono et al., 2014a; Di Genova et al., 2016), and confirm Arrhenian behavior, highlighting the important effect of the alkali elements on the rheology of molten carbonates at upper mantle conditions. We find that, molten Na_2CO_3 provides a valid analogue for investigating the rheology of carbonatitic magmas at high pressure, and can help to better understand the role of alkali on the migration rate of CO_2-rich magmas at mantle conditions. The relatively low ascent rate of carbonatitic melts is consistent with the presence of low seismic velocity zones detected beneath mid -ocean ridges, as well as their presence as melt inclusions in lithospheric fibrous diamonds.

Acknowledgments

V.S. gratefully acknowledges financial support from PRIUS program (GRC, Ehime University) and the Deep Carbon Observatory. This work was performed at HPCAT (Sector 16), Advanced Photon Source (APS), Argonne National Laboratory. HPCAT operation is supported by DOE-NNSA under Award No. DE-NA0001974, with partial instrumentation funding by NSF. The Advanced Photon Source is a U.S. Department of Energy (DOE) Office of Science User Facility operated for the DOE Office of Science by Argonne National Laboratory under Contract No. DE-AC02-06CH11357. Y.K. acknowledges the support of DOE-BES/DMSE under Award DE-FG02-99ER45775 and support by the National Science Foundation under Award No. EAR-1722495. An early version of this manuscript benefited from critical comments by Michele Lustrino. We thank two anonymous reviewers for their constructive comments.

Appendix A. Supplementary data

Supplementary data to this article can be found online at https://doi.org/10.1016/j.chemgeo.2018.09.036.

References

Aulbach, S., Stagno, V., 2016. Evidence for a reducing Archean ambient mantle and its effects on the carbon cycle. Geology 44, 751–754.
Besson, J.M., Nelmes, R.J., Hamel, G., Loveday, J.S., Weill, G., Hull, S., 1992. Neutron powder diffraction above 10 GPa. Phys. B Condens. Matter 180–181 (Part 2), 907–910.
Chantel, J., Manthilake, G., Andrault, D., Novella, D., Yu, T., Wang, Y., 2016. Experimental evidence supports mantle partial melting in the asthenosphere. Sci. Adv. 2, e1600246.
Dalton, J.A., Presnall, D.C., 1998. The continuum of primary carbonatitic-kimberlitic melt compositions in equilibrium with lherzolite: data from the system CaO-MgO-Al_2O_3-SiO_2-CO_2 at 6 GPa. J. Petrol. 39, 1953–1964.
Dalton, J.A., Wood, B.J., 1993. The compositions of primary carbonate melts and their evolution through wallrock reaction in the mantle. Earth Planet. Sci. Lett. 119, 511–525.
Dasgupta, R., Hirschmann, M.M., 2010. The deep carbon cycle and melting in Earth's interior. Earth Planet. Sci. Lett. (Frontiers) 298, 1–13.
Dasgupta, R., Hirschmann, M.M., McDonough, W.F., Spiegelman, M., Withers, A.C., 2009. Trace element partitioning between garnet lherzolite and carbonatite at 6.6 and 8.6 GPa with applications to the geochemistry of the mantle and of mantle-derived melts. Chem. Geol. 262, 57–77.
Dasgupta, R., Mallik, A., Tsuno, K., Withers, A.C., Hirth, G., Hirschmann, M.M., 2013. Carbon-dioxide-rich silicate melt in the Earth's upper mantle. Nature 493, 211–215.
Di Genova, D., Cimarelli, C., Hess, K., Dingwell, D.B., 2016. An advanced rotational rheometer system for extremely fluid liquids up to 1273 K and applications to alkali carbonate melts. Am. Mineral. 101, 953–959.
Dingwell, D., 2006. Transport properties of magmas: diffusion and rheology. Elements 2, 281–286.
Dobson, D.P., Jones, A.P., Rabe, R., Sekine, T., Kurita, K., Taniguchi, T., Kondo, T., Kato, T., Shimomura, O., Urakawa, S., 1996. In-situ measurement of viscosity and density of carbonate melts at high pressure. Earth Planet. Sci. Lett. 143, 207–215.
Dorogokupets, P.I., Dewaele, A., 2007. Equations of state of MgO, Au, Pt, NaCl-B1, and NaCl-B2: internally consistent high-temperature pressure scales. High Pressure Res. 27, 431–446.
Dunn, R.A., Toomey, D.R., Detrick, R.S., Wilcock, W.S.D., 2001. Continuous mantle melt supply beneath an overlapping spreading center on the East Pacific Rise. Science 291, 1955–1958.
Eggler, D.H., Baker, D.R., 1982. Reduced volatiles in the system C-O-H: implications to mantle melting, fluid formation, and diamond genesis. High-Press. Res. Geophys. 237–250.
Evans, R.L., Tarits, P., Chave, A.D., White, A., Heinson, G., Filloux, J.H., Toh, H., Seama, N., Utada, H., Booker, J.R., Unsworth, M.J., 1999. Asymmetric electrical structure in the mantle beneath the east Pacific rise at 17S. Science 286, 752–756.

Gaillard, F., Malki, M., Iacono-Marziano, G., Pichavant, M., Scaillet, B., 2008. Carbonatite melts and electrical conductivity in the asthenosphere. Science 322, 1363–1365.
Genge, M.J., Price, G.D., Jones, A.P., 1995. Molecular dynamics simulations of $CaCO_3$ melts to mantle pressures and temperatures: implications for carbonatite magmas. Earth Planet. Sci. Lett. 131, 225–238.
Giordano, D., Mangiacapra, A., Potuzak, M., Russell, J.K., Romano, C., Dingwell, D.B., Di Muro, A., 2006. An expanded non-Arrhenian model for silicate melt viscosity: a treatment for metaluminous, peraluminous and peralkaline liquids. Chem. Geol. 229, 42–56.
Giuliani, A., Kamenetsky, V.S., Phillips, D., Kendrick, M.A., Wyatt, B.A., Goemann, K., 2012. Nature of alkali-carbonate fluids in the sub-continental lithospheric mantle. Geology 40, 967–970.
Gu, Y.J., Lerner-Lam, A.L., Dziewonski, A.M., Ekstrom, G., 2005. Deep structure and seismic anisotropy beneath the East Pacific Rise. Earth Planet. Sci. Lett. 232, 259–272.
Gudfinnsson, G.H., Presnall, D.C., 2005. Continuous gradations among primary kimberlitic, carbonatitic, melilitic, basaltic, picritic, and komatiitic melts in equilibrium with garnet lherzolite at 3-8 GPa. J. Petrol. 46, 1645–1659.
Hammouda, T., Keshav, S., 2015. Melting in the mantle in the presence of carbon: Review of experiments and discussion on the origin of carbonatites. Chem. Geol. 418, 171–188.
Hammouda, T., Laporte, D., 2000. Ultrafast mantle impregnation by carbonatite melts. Geology 28, 283–285.
Hudspeth, J., Sanloup, C., Kono, Y., 2018. Properties of molten $CaCO_3$ at high pressure. Geochem. Perspect. Lett. 7, 17–21.
Irving, A.J., Wyllie, P.J., 1975. Subsolidus and melting relationships for calcite, magnesite and the join $CaCO_3$-$MgCO_3$ 36 kb. Geochim. Cosmochim. Acta 39, 35–53.
Kamenetsky, V.S., Yaxley, G.M., 2015. Carbonate-silicate liquid immiscibility in the mantle propels kimberlite magma ascent. Geochim. Cosmochim. Acta 158, 48–56.
Kamenetsky, V.S., Grütter, H., Kamenetsky, M.B., Gömann, K., 2013. Parental carbonatitic melt of the Koala kimberlite (Canada): constraints from melt inclusions in olivine and Cr-spinel, and groundmass carbonate. Chem. Geol. 353, 96–111.
Kamenetsky, V.S., Belousova, E.A., Giuliani, A., Kamenetsky, M.B., Goemann, K., Griffin, W.L., 2014. Chemical abrasion of zircon and ilmenite megacrysts in the Monastery kimberlite: implications for the composition of kimberlite melts. Chem. Geol. 383, 76–85.
Kanzaki, M., Kurita, K., Fujii, T., Kato, T., Shimomura, O., Akimoto, S., 1987. A new technique to measure viscosity and density of silicate melts at high pressure. In: Manghnani, M.H., Syono, Y. (Eds.), High-pressure Research in Mineral Physics. America Geophysical Union, Washington, D.C., pp. 195–200.
Keller, T., Katz, R.F., Hirschmann, M.M., 2017. Volatiles beneath mid-ocean ridges: deep melting, channelised transport, focusing, and metasomatism. Earth Planet. Sci. Lett. 464, 55–68.
Klotz, S., Hamel, G., Frelat, J., 2004. A new type of compact large-capacity press for neutron and x-ray scattering. High Pressure Res. 24, 219–223.
Kono, Y., Irifune, T., Higo, Y., Inoue, T., Barnhoorn, A., 2010. P-V-T relation of MgO derived by simultaneous elastic wave velocity and in situ X-ray measurements: a new pressure scale for the mantle transition region. Phys. Earth Planet. Inter. 183, 196–211.
Kono, Y., Kenney-Benson, C., Park, C., Shen, G., Wang, Y., 2013. Anomaly in the viscosity of liquid KCl at high pressures. Phys. Rev. B 87, 024302.
Kono, Y., Kenney-Benson, C., Hummer, D., Ohfuji, H., Park, C., Shen, G., Wang, Y., Kavner, A., Manning, C.E., 2014a. Ultralow viscosity of carbonate melts at high pressures. Nat. Commun. 5, 5091.
Kono, Y., Park, C., Kenney-Benson, C., Shen, G., Wang, Y., 2014b. Toward comprehensive studies of liquids at high pressures and high temperatures: combined structure, elastic wave velocity, and viscosity measurements in the Paris-Edinburgh cell. Phys. Earth Planet. Inter. 228, 269–280.
Kopylova, M., Navon, O., Dubrovinsky, L., Khachatryan, G., 2010. Carbonatitic mineralogy of natural diamond-forming fluids. Earth Planet. Sci. Lett. 291, 126–137.
Li, Z., Li, J., Lange, R., Liu, J., Militzer, B., 2017. Determination of calcium carbonate and sodium carbonate melting curves up to Earth's transition zone pressures with implications for the deep carbon cycle. Earth Planet. Sci. Lett. 457, 395–402.
Litasov, K.D., Ohtani, E., 2009a. Phase relations in the peridotite-carbonate-chloride system at 7.0–16.5 GPa and the role of chlorides in the origin of kimberlite and diamond. Chem. Geol. 262, 29–41.
Litasov, K.D., Ohtani, E., 2009b. Solidus and phase relations of carbonated peridotite in the system CaO-Al_2O_3-MgO-SiO_2-Na_2O-CO_2 to the lower mantle depths. Phys. Earth Planet. Inter. 177, 46–58.
Litasov, K.D., Ohtani, E., 2010. The solidus of carbonated eclogite in the system CaO-Al_2O_3-MgO-SiO_2-Na_2O-CO_2 to 32 GPa and carbonatite liquid in the deep mantle. Earth Planet. Sci. Lett. 295, 115–126.
Litasov, K.D., Shatskiy, A., Ohtani, E., Yaxley, G.M., 2013. The solidus of alkaline carbonatite in the deep mantle. Geology 41, 79–82.
Litasov, K.D., Shatskiy, A., Ohtani, E., 2014. Melting and subsolidus phase relations in peridotite and eclogite systems with reduced C-O-H fluid at 3–16 GPa. Earth Planet. Sci. Lett. 391, 87–99.
Liu, Q., Lange, R.A., 2003. New density measurements on carbonate liquids and the partial molar volume of the $CaCO_3$ component. Contrib. Mineral. Petrol. 146, 370–381.
Maude, A.D., 1961. End effects in a falling-sphere viscometer. Br. J. Appl. Phys. 12, 293–295.
Minarik, W.G., Watson, E.B., 1995. Interconnectivity of carbonate melt at low melt fraction. Earth Planet. Sci. Lett. 133, 423–437.
Rohrbach, A.C., Schmidt, M.W., 2011. Redox freezing and melting in the Earth's deep mantle resulting from carbon-iron redox coupling. Nature 472, 209–212.
Russell, J.K., Porritt, L.A., Lavallee, Y., Dingwell, D.B., 2012. Kimberlite ascent by assimilation-fuelled buoyancy. Nature 481, 352–356.
Salters, V.J.M., Hart, S.R., 1989. The Hf-paradox, and the role of garnet in the MORB source. Nature 342, 420–422.
Shatskiy, A., Borzdov, Y.M., Litasov, K.D., Sharygin, I.S., Palyanov, Y.N., Ohtani, E., 2015. Phase relationships in the system K_2CO_3-$CaCO_3$ at 6 GPa and 900–1450 °C. Am. Miner. 100, 223–232.
Shiryaev, A.A., Izraeli, E.S., Hauri, E., Zakharchenko, O.D., Navon, O., 2005. Chemical, optical, and isotopic investigations of fibrous diamonds from Brazil. Russ. Geol. Geophys. 46, 1207–1222.
Stagno, V., Frost, D.J., 2010. Carbon speciation in the asthenosphere: experimental measurements of the redox conditions at which carbonate-bearing melts coexist with graphite or diamond in peridotite assemblages. Earth Planet. Sci. Lett. 30, 72–84.
Stagno, V., Ojwang, D.O., McCammon, C.A., Frost, D.J., 2013. The oxidation state of the mantle and the extraction of carbon from Earth's interior. Nature 11679, 493.
Stagno, V., Frost, D.J., McCammon, C.A., Mohseni, H., Fei, Y., 2015. The oxygen fugacity at which graphite or diamond forms from carbonate-bearing melts in eclogitic rocks. Contrib. Mineral. Petrol. 169, 16.
Suito, K., Namba, J., Horikawa, T., Taniguchi, Y., Sakurai, N., Kobayashi, M., Onodera, A., Shimomura, O., Kikegawa, T., 2001. Phase relations of CaCO3 at high pressure and high temperature. Am. Mineral. 86, 997–1002.
Terasaki, H., Kato, T., Urakawa, S., Funakoshi, K.I., Suzuki, A., Okada, T., ... Kasai, S., 2001. The effect of temperature, pressure, and sulfur content on viscocity of the Fe-FeS melt. Earth Planet. Sci. Lett. 190 (1–2), 93–101.
Thomson, A.R., Walter, M.J., Kohn, S.C., Brooker, R.A., 2016. Slab melting as a barrier to deep carbon subduction. Nature 529, 76–79.
Watson, E.B., Brenan, J.M., Baker, D.R., 1990. Distribution of fluids in the continental mantle. In: Menzies, M.A. (Ed.), Continental Mantle: Oxford Monographs on Geology and Geophysics. 16. pp. 111–125.
Wolff, J.A., 1994. Physical properties of carbonatite magmas inferred from molten salt data, and application to extraction patterns from carbonatite–silicate magma chambers. Geol. Mag. 131, 145–153.
Woodland, A.B., Koch, M., 2003. Variation in oxygen fugacity with depth in the upper mantle beneath Kaapvaal craton, South Africa. Earth Planet. Sci. Lett. 214, 295–310.
Woolley, A.R., Kjarsgaard, B.A., 2008. Carbonatite occurrences of the world: map and database. In: Geological Survey of Canada, Open File 5796, 1 CD-ROM + 1 Map.